

**Black hole from merging binary neutron stars: How fast can it spin?**Wolfgang Kastaun,<sup>1</sup> Filippo Galeazzi,<sup>2,1</sup> Daniela Alic,<sup>1</sup> Luciano Rezzolla,<sup>1</sup> and José A. Font<sup>2</sup><sup>1</sup>*Max-Planck-Institut für Gravitationsphysik, Albert-Einstein-Institut, Potsdam 14476, Germany*<sup>2</sup>*Departamento de Astronomía y Astrofísica, Universitat de València, Dr. Moliner 50, 46100 Burjassot (València), Spain*

(Received 1 February 2013; published 2 July 2013)

The merger of two neutron stars will in general lead to the formation of a torus surrounding a black hole whose rotational energy can be tapped to potentially power a short gamma-ray burst. We have studied the merger of equal-mass binaries with spins aligned with the orbital angular momentum to determine the maximum spin the black hole can reach. Our initial data consists of irrotational binaries to which we add various amounts of rotation to increase the total angular momentum. Although the initial data violates the constraint equations, the use of the constraint-damping conformal and covariant Z4 formulation yields evolutions with violations smaller than those with irrotational initial data and standard formulations. Interestingly, we find that a limit of  $J/M^2 \simeq 0.89$  exists for the dimensionless spin and that any additional angular momentum given to the binary ends up in the torus rather than in the black hole, thus providing another nontrivial example supporting the cosmic censorship hypothesis.

DOI: [10.1103/PhysRevD.88.021501](https://doi.org/10.1103/PhysRevD.88.021501)

PACS numbers: 04.25.dk, 04.25.Nx, 04.30.Db, 04.40.Dg

**I. INTRODUCTION**

A long-standing open question in general relativity is how close the angular momentum  $J_{\text{BH}}$  of a black hole (BH) created in astrophysical scenarios can get to the theoretical maximum, which for an isolated BH is  $M_{\text{ADM}}^2$  (throughout this paper we use geometric units unless noted otherwise), with  $M_{\text{ADM}}$  the ADM mass. Under very general conditions, the limit is  $A/(8\pi)$ , with  $A$  the horizon area [1]. So far, no violation of the cosmic censorship hypothesis, i.e., no formation of a naked singularity, has been found in numerical simulations evolving generic initial data satisfying the dominant energy condition (but see also Ref. [2]). This question has been studied for the collapse of supermassive stars, e.g., Ref. [3]; neutron stars (NSs) with  $J_{\text{NS}}/M_{\text{NS}}^2 > 1$  [4]; for the merger of binary NSs (BNSs), e.g., Refs. [5–7]; of BH-NS binaries, e.g., Ref. [8]; and of BH binaries, e.g., Ref. [9]. In all cases investigated, the final BH spin is below the critical value, and semianalytical estimates seem to indicate this is true for all configurations [10,11].

Determining the final spin produced in the merger of BNSs is not a mere academic question as the rapid rotation of the BH is a key ingredient in all of the models in which the BNS merger is thought to lead to a jet formation and a short gamma-ray burst [12–14]. Because the energetics of the emission will depend sensitively on the BH spin, an accurate measure of the maximum value attainable can help set upper limits on the efficiency of the process (see Ref. [15] for a recent discussion and a list of references). Despite its importance, this issue has not been addressed yet, and the main reason is the lack of constraint-satisfying initial data for spinning NSs. Early attempts to construct such initial data, e.g., Refs. [16,17], did not have a satisfactory solution of the Euler equation according to Ref. [18]. Only recently, initial data for BNSs with spins

has been computed [19], but no evolutions have been reported yet.

Here we follow a novel approach, which consists of setting up constraint-violating initial data by adding a rotational velocity field to self-consistent irrotational initial data and then evolving with a recently developed constraint-damping conformal and covariant Z4 (CCZ4) formalism [20]. We show that this choice reduces the constraint violations quickly to a level which is even smaller than the one encountered in BNS evolutions of irrotational initial data with standard formulations. The drawback of this simple method is that the artificial spin-up also introduces oscillations of the star and eccentricity of the orbit. This would be unacceptable for modelling gravitational-wave emission, but it is adequate to assess the influence of the NS spin on the BH.

**II. BINARY INITIAL DATA WITH SPIN**

The best way to decide what are realistic expectations for the spin in merging BNSs is to look at the available observations. Although the distribution of NS spins is still unknown, NSs at birth are expected to have spins in the range of 10–140 ms [21], and dimensionless spin parameters  $J_{\text{NS}}/M_{\text{NS}}^2 \sim 1$  should be attainable only by millisecond pulsars that have been spun up by accretion [22]. It is, however, unlikely that the old NSs of a binary system which is about to merge have periods less than 1 ms, and all the observational evidence supports this conclusion. We know, in fact, that the period of the fastest known pulsar in a BNS system, J0737-3039A, is 22.70 ms, yielding a dimensionless spin parameter  $J_{\text{NS}}/M_{\text{NS}}^2 \sim 0.05$  [23]. In view of these considerations, we restrict our analysis to binaries  $-0.2 \lesssim J_{\text{NS}}/M_{\text{NS}}^2 \lesssim 0.3$ , thus well within the range of realistic possibilities.

To construct initial data for a binary system of spinning NSs, we modify the velocity field of the irrotational equal mass solutions computed using the LORENE code [24]. We set  $\vec{w} = (1 - s)\vec{w}_L + s\vec{\Omega} \times \vec{x}$ , where  $w^i = u^i/u^0$  denotes the coordinate velocity of the fluid in the star,  $u^\mu$  the fluid 4-velocity,  $\vec{\Omega}$  the orbital angular velocity vector,  $\vec{w}_L$  is the original irrotational velocity field, and  $s$  is a free parameter we tune to increase/decrease the spin of the star  $J_{\text{NS}}$  ( $s = 0$  corresponds to a purely irrotational binary,  $s = 1$  to a corotating one). Once a spin-up/-down is introduced, we parametrize a binary in terms of the additional ADM angular momentum it has with respect to the irrotational model,  $\Delta J_{\text{ADM}}$ . Note we compute  $J_{\text{ADM}}$  using Eq. (68) of Ref. [24] because this form is more robust against constraint violations. Two remarks should be made on our prescription for  $\vec{w}$ . First, it corresponds to stars with spins aligned with the orbital angular momentum, which is the most relevant case for our goals, since it leads to the maximum increase of total angular momentum. Second, it guarantees that the residual vector field is orthogonal to the density gradient, and hence the flow is adapted to the deformed shape of the stars in the binary. However, because the hydrostatic equations are no longer satisfied with the new velocity field, it introduces oscillations in the stars as they are evolved. The relative variation of the central rest-mass density stays below 1% for the irrotational models, is  $\leq 8\%$  for  $s = 0.85$  and  $\leq 15\%$  for the extreme case of  $s = 1.2$ .

Using the above method, we construct sequences of increasing spin, each with a fixed baryon mass, from  $1.625M_\odot$  to  $1.901M_\odot$  for each star, and the same initial separation of 45 km, which corresponds to roughly 3 orbits until merger for the irrotational case (up to 4 for the fastest spinning cases). The stars obey initially a polytropic equation of state (EOS)  $P(\rho) = K\rho^\Gamma$  with  $\Gamma = 2$  and  $K = 123.6$  in units in which  $G = c = M_\odot = 1$ . During the evolution, however, we use an ideal-fluid ( $\Gamma$ -law) EOS [5] with  $\Gamma = 2$ . Since we are interested in the *maximum* spin of the BH, we focus on binaries that will collapse promptly as any intervening long-lived hypermassive neutron star would just extract additional angular momentum from the system. Hence, we consider only models with total baryon masses well above the maximum one for a nonrotating star, which for our EOS is  $2.0M_\odot$ . We increase the spin frequency up to 55% of the Kepler limit, which corresponds to  $s = 1.2$ , but larger values are possible in principle. As in our previous work (e.g., Ref. [25]), we use adaptive mesh-refinement techniques [26] with 6 levels during inspiral, two of which follow the stars, and a 7th finest level activated at the time of collapse. The outer boundary is located at 756 km, where Sommerfeld radiation boundary conditions are applied.

### III. CCZ4 AND BSSNOK FORMULATIONS

We have already mentioned the importance of using a formulation of the Einstein equations that damps rapidly

the violations of the constraints caused by our modifications of the initial data. To achieve this, we employ the recently proposed CCZ4 formalism [20] and couple it to the equations of relativistic hydrodynamics. We have carried out a systematic investigation of this new formulation in comparison with the more standard Baumgarte-Shapiro-Shibata-Nakamura-Oohara-Kojima (BSSNOK) one [27,28], including the evolution of a stable isolated NS, the collapse of an unstable star to a BH, and the merger of BNSs in quasicircular and eccentric orbits. For lack of space, these tests will be presented in detail in a forthcoming longer publication, and here we restrict the discussion to the constraint-damping properties of the CCZ4. The comparison reveals not only the advantages of the CCZ4 formulation over BSSNOK, but it also provides a way to estimate how much constraint violations are tolerable before the influence on the dynamics becomes significant, by looking at the difference between two simulations of the same system with very different constraint violations. More specifically, we can start assessing the role played by the initial constraint violations with the extreme case of an eccentric binary as created from quasicircular initial data in which we reduce artificially the linear momenta by 15%. Doing this induces very large constraint violations in both formulations, although the  $L_2$  norm of the Hamiltonian constraint in CCZ4 evolutions always becomes smaller by a factor of 5–10. Not surprisingly, the dynamics of the system shows large differences in the phase evolution and in the trajectories, demonstrating that the initial constraint violations are too high to yield meaningful results. On the other hand, for quasicircular binaries, the orbital trajectories for CCZ4 and BSSNOK agree quite well, with a phase error of 4%. At the time of merger, the mass and the spin of the BH agree within 0.6% and 0.4%, which is less than our estimate of 1% for the numerical errors. Again, we find that the use of CCZ4 reduces the  $L_2$  norm of the Hamiltonian constraint, on average by 1 order of magnitude. In particular, a very sharp decrease is seen during the first millisecond (cf. left panel of Fig. 1). Under similar but not identical conditions, Ref. [29] has reported a larger decrease for an alternative conformal formulation of the Z4 system, Z4c. Without a direct comparison, it is difficult to assess why it results in a smaller violation. It may also be due to the improved treatment of the outer boundaries in Ref. [29].

A similar behavior is also observed for NSs that are spun up/down. This is shown in the left part of Fig. 1, which reports the evolution of the  $L_2$  norm for a number of binaries with different degrees of spin-up/-down, when evolved with either the CCZ4 or the BSSNOK formulation. The initial violation is obviously larger for larger changes of spin, but in all CCZ4 evolutions, the violation is reduced by about 1 order of magnitude after 1 ms, becoming less than the one from BSSNOK evolutions with constraint-satisfying initial data. Afterward, the constraints exhibit

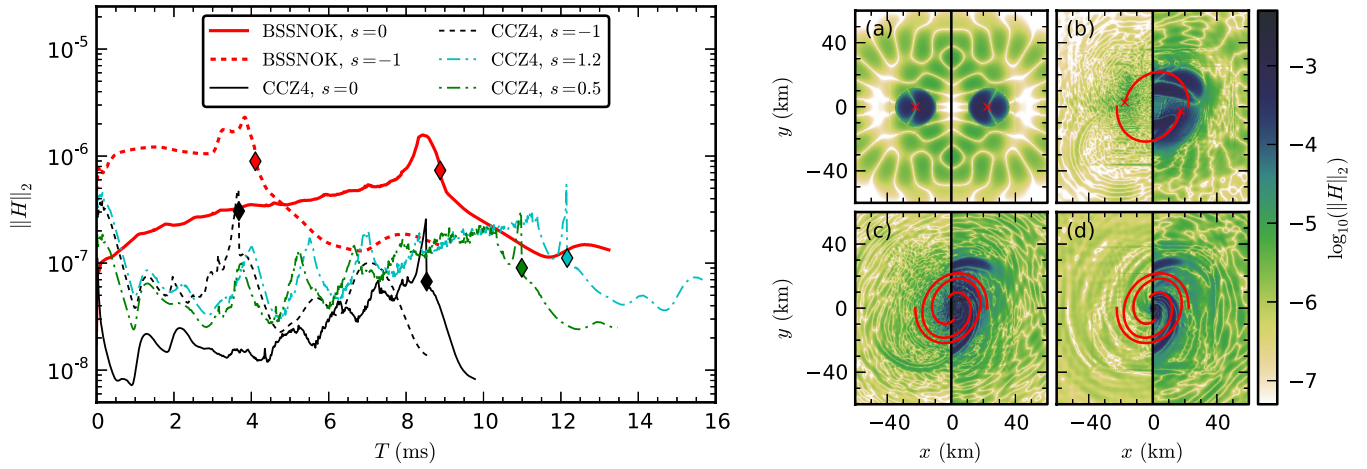


FIG. 1 (color online). Left: Time evolution of the  $L_2$  norm of the Hamiltonian constraint  $H$  over the whole domain, excluding the AH, obtained using CCZ4 and BSSNOK formulations. The symbols mark the AH formation. Right: Snapshots in the orbital plane for  $s = -1$ , at times (a)  $t = 0$ ; (b)  $t = 1.48$  ms, during inspiral; (c)  $t = 3.48$  ms, shortly before horizon formation; and (d)  $t = 4.46$  ms, shortly after. The left half of each panel shows the  $L_2$  norm of  $H$  as obtained with CCZ4 evolutions, the right half with BSSNOK. The red solid lines mark the trajectories of the NSs. In all cases the binaries have  $M_{\text{NS}} = 1.78M_{\odot}$ .

the usual behavior resulting from the interplay between constraint-violating numerical errors and the action of the damping terms in the CCZ4 system [20], resulting in a series of maxima and minima. This behavior should be contrasted with the one of the BSSNOK formulation, where the constraints instead remain large during the whole evolution. For the latter, the errors tend to accumulate at each point in space, causing the stars to leave behind lumps of constraint violations. This is shown in the right part of Fig. 1, which displays the Hamiltonian constraint violation at different stages of the evolution for the case  $s = -1$ , both for CCZ4 and BSSNOK. The comparison highlights that while the constraint violations are damped/propagated away in the CCZ4 evolution, they remain static in the BSSNOK one.

Interestingly, even with the most severe spin change of the  $s = -1$  binary, the violation with the CCZ4 formulation is smaller by a factor of  $\sim 5$  than the one obtained with the BSSNOK formulation for irrotational binaries (red solid line), which represents the best-case for that formulation. Therefore, since in all CCZ4 evolutions the constraint violations fall below the irrotational case with BSSNOK, we conclude that after the first millisecond, the errors due to constraint violations are comparable with the differences between BSSNOK and CCZ4 in the irrotational case. Furthermore, to assess also the influence of the large violation during the first millisecond, we note that for the case  $s = -1$ , the difference in BH mass, spin, and merger time between BSSNOK and CCZ4 evolutions are 0.7%, 3%, and 10%, respectively. Since CCZ4 evolutions always have smaller violations after the first millisecond, we conclude that the error in the BH mass and spin due to constraint violations is less than 1%, and the total error, including the numerical one, is less than 2%.

We note that the action of the constraint-damping CCZ4 formulation is that of mapping the constraint-violating initial data closer to the space of self-consistent solutions of the Einstein-Euler equations. This mapping is active throughout the evolution and not only during the first millisecond, although that is when it is most evident. We also note that the use of constraint-violating initial data inevitably also changes the physical parameters of the system, such as the eccentricity and the hydrostatic equilibrium (which is perturbed). Although we lose a certain amount of control over the physical parameters of the system this way, part of the uncertainty also comes from the fact that the added rotational velocity field affects also other physical quantities besides the intended one, which is the spin. It is for those reasons that we cannot prescribe the physical properties of our initial data exactly. The uncertainty introduced is larger for systems with the largest spins. This is why our simulations cannot be used for a reliable description of gravitational wave forms and why we do not consider stars spinning near the Kepler limit. However, because our goal here is to show that a limit exists to the maximum spin of the black hole, we are not particularly concerned whether our initial data corresponds exactly to a particular configuration as long as it is physically consistent.

#### IV. FINAL BH SPIN

We turn now to discuss our physical results and their astrophysical implications. We first note that for the lightest binary ( $M_{\text{NS}} = 1.63M_{\odot}$ ), only the irrotational model forms a BH promptly, while a hypermassive neutron star is formed for  $s = 0.5, 1.2$ . This is not unexpected but highlights that if the total mass is close to the critical mass for a



prompt collapse, the spin of the NSs can have a strong impact on the dynamics of the merger and thus on the gravitational-wave signal. For the heavier binaries, instead, we observe the immediate formation of a BH and a torus. Quasistationarity is reached soon after merger, with the BH mass and spin changing less than 0.4% during the last  $50M_{\text{BH}}$  for all simulations and with negligible mass accretion. These conditions are essential to use the isolated-horizon formalism to measure the properties of the BH.

To measure the contribution to the total angular momentum of the fluid orbiting outside the BH, we monitor the quantity  $J_{\text{F}} \equiv - \int_{V_o} d^3V n^\mu \phi^\nu T_{\mu\nu}$ , where  $V_o$ ,  $d^3V$ ,  $n^\mu$ ,  $T_{\mu\nu}$  denote, respectively, the portion of the time slice  $\Sigma_t$  outside the apparent horizon (AH), the proper volume element, the unit normal to  $\Sigma_t$ , the energy-momentum tensor, and  $\phi \equiv \partial_\phi$  is the basis vector of the spherical coordinate system obtained from the Cartesian one used in the simulations.  $J_{\text{F}}$  reduces to the angular momentum in the Newtonian limit but is not conserved unless  $\phi$  is a Killing vector (in which case it is conserved even for nonaxisymmetric flows [30]) and coincides with the Komar angular momentum for stationary axisymmetric spacetimes. We define the angular momentum of the torus  $J_{\text{T}}$  as the angular momentum  $J_{\text{F}}$  of the fluid at the end of the simulation, when the BH has become stationary and mass accretion is negligible.

On the other hand, to measure the angular momentum of the BH, we use the isolated-horizon formalism [31,32], computing the integral  $J_{\text{BH}}(t) \equiv (8\pi)^{-1} \int_{A_t} d^2V \Phi^\mu R^\nu K_{\mu\nu}$  on the AH surface  $A_t$ , where  $\Phi^\mu$ ,  $R^\nu$ ,  $K_{\mu\nu}$  are, respectively, an (approximate) axial Killing vector on the AH, the unit normal to  $A_t$  on  $\Sigma_t$ , and the extrinsic curvature. Surprisingly, the sum of  $J_{\text{F}}$  and  $J_{\text{BH}}$  at the end of the simulations agrees with  $J_{\text{F}}$  at the time of AH formation to better than 2.2% on average, with a variance  $\approx 0.5\%$  during the whole time from the formation of the horizon until stationarity (the surprise comes from the fact that  $J_{\text{F}}$ , which is not expected to be conserved in general, nevertheless represents a rather useful measure at the time the black hole is formed). This behavior can be explained using Eq. (45) in Ref. [33], which indicates that the time derivative of this sum is small if  $\phi^\mu$  becomes approximately a Killing vector of the spacetime and the gravitational-wave emission from the AH is small. Both conditions are satisfied at the time of horizon formation to a degree sufficient for us to use  $J_{\text{F}}$  at this time to estimate the final total angular momentum.

The results of our simulations are summarized in the left panel of Fig. 2, which reports with filled symbols the dimensionless spin of the BH,  $J_{\text{BH}}/M_{\text{BH}}^2$ . Note that  $M_{\text{BH}}$  is the horizon mass [32] computed from  $J_{\text{BH}}$  and the horizon area using the Kerr formula so that the extremal case  $8\pi J_{\text{BH}} = A$  [1] is equivalent to  $J_{\text{BH}} = M_{\text{BH}}^2$ . The data are presented as a function of the (dimensionless) additional

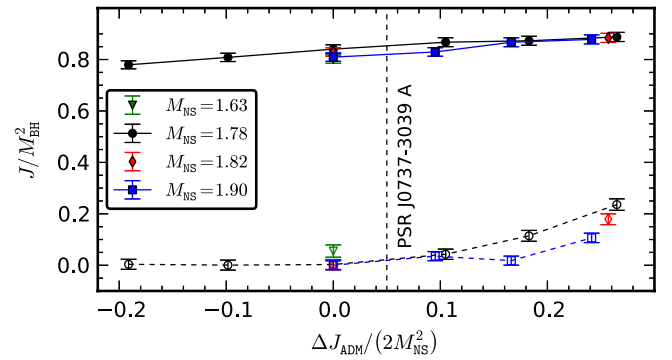


FIG. 2 (color online). Dimensionless spin of the BH  $J_{\text{BH}}/M_{\text{BH}}^2$  (filled symbols) and of the torus  $J_{\text{T}}/M_{\text{BH}}^2$  (empty symbols) versus the additional initial angular momentum  $\Delta J_{\text{ADM}}$ . The error bars include discretization errors and the influence of the constraint violations.

initial angular momentum per star,  $\frac{1}{2} \Delta J_{\text{ADM}}/M_{\text{NS}}^2$ , relative to the corresponding irrotational model. Values of  $\Delta J_{\text{ADM}}/M_{\text{NS}}^2 \geq 0$  correspond to an increase of total angular momentum, while  $\Delta J_{\text{ADM}}/M_{\text{NS}}^2 \leq 0$  to NSs with antialigned spins. For comparison, we also plot the estimate for the dimensionless spin of PSR J0737-3039A.

As it is natural to expect, the BH spin increases with the initial total angular momentum of the binary, and for a binary like PSR J0737-3039A, it is not much larger than for an irrotational one. Surprisingly, however, the growth is not constant and actually saturates for  $\Delta J_{\text{ADM}}/M_{\text{NS}}^2 \approx 0.2$ , quite independently of the initial (baryon) mass in the binary. The largest BH spin we obtain is  $J_{\text{BH}}/M_{\text{BH}}^2 = 0.888 \pm 0.018$  for  $M_{\text{NS}} = 1.78M_{\odot}$  and  $s = 1.2$ . At the same time, we also find that the combined angular momentum of the BH and of the torus,  $J_{\text{tot}} = J_{\text{BH}} + J_{\text{T}}$ , continues to increase for all values of  $s$  used. More precisely, for  $s \leq 1$ , the increase is essentially linear, with  $J_{\text{tot}} = J_{\text{tot}}^{\text{irrot}} + \eta \Delta J_{\text{ADM}}$ , where  $\eta = 0.55(0.60)$  for  $M_{\text{NS}} = 1.78(1.90)M_{\odot}$  and  $J_{\text{tot}}^{\text{irrot}}$  is the value of  $J_{\text{tot}}$  for the irrotational binary. This means that roughly half of the additional angular momentum has been radiated as gravitational waves (see Ref. [34] for a detailed discussion of the angular momentum radiated in gravitational waves for simulations similar to the ones discussed here). For sufficiently large spin-ups, a significant fraction of the remaining angular momentum is transferred to the torus, which therefore acts as the channel absorbing the excess angular momentum and limits the spin-up of the BH. This is reported in Fig. 2, which shows that  $J_{\text{T}}$  (empty symbols) is very small for antialigned spins and irrotational binaries but increases rapidly with the initial stellar spin.

Of course it is difficult to provide a simple explanation for this nonlinear behavior, although one might speculate that spinning up the NSs will provide matter with sufficient angular momentum to then produce a torus. Overall, however, our results provide another nontrivial example that, as

proposed by the cosmic censorship hypothesis, a self-consistent evolution of the Einstein equations from generic initial conditions leads to a BH formation rather than a naked singularity.

We will conclude with a few remarks. First, it is reasonable that the material in the torus will eventually be accreted onto the BH, transferring angular momentum and further increasing the BH spin. However, this will happen on dissipative time scales which are longer and thus not relevant for the central engine of gamma-ray bursts, which should be ignited on a dynamical time scale after the merger. The tori produced in these simulations, in fact, are expected to be accreted on a timescale of  $\sim 0.3$  s [14] (Ref. [34] indicates that the accretion time scale becomes even larger for the case of unequal masses). Second, because magnetic fields are expected to further decrease the angular momentum in the system, they are not

particularly relevant in our considerations, which focus on the maximum spin in a prompt BH formation. Finally, although the BH spin seems to increase for irrotational unequal masses [34], the spin could also decrease depending on the amount of mass and spin in the torus. In any case, we expect an upper limit will be found also for generic binaries, and this will be the focus of our future work.

## ACKNOWLEDGMENTS

Support comes through the DFG grant SFB/Trans-regio 7, “CompStar”, a Research Networking Programme of the ESF and the Spanish MICINN (Grant No. AYA 2010-21097-C03-01). F. G. is supported by a VESF fellowship from the European Gravitational Observatory (Grant No. EGO-DIR-69-2010).

- 
- [1] J. L. Jaramillo, M. Reiris, and S. Dain, *Phys. Rev. D* **84**, 121503 (2011).
  - [2] T. Bode, P. Laguna, and R. Matzner, *Phys. Rev. D* **84**, 064044 (2011).
  - [3] M. Saijo and I. Hawke, *Phys. Rev. D* **80**, 064001 (2009).
  - [4] B. Giacomazzo, L. Rezzolla, and N. Stergioulas, *Phys. Rev. D* **84**, 024022 (2011).
  - [5] L. Baiotti, B. Giacomazzo, and L. Rezzolla, *Phys. Rev. D* **78**, 084033 (2008).
  - [6] K. Kiuchi, Y. Sekiguchi, M. Shibata, and K. Taniguchi, *Phys. Rev. D* **80**, 064037 (2009).
  - [7] R. Gold, S. Bernuzzi, M. Thierfelder, B. Brüggmann, and F. Pretorius, *Phys. Rev. D* **86**, 121501 (2012).
  - [8] K. Kyutoku, H. Okawa, M. Shibata, and K. Taniguchi, *Phys. Rev. D* **84**, 064018 (2011).
  - [9] I. Hinder, B. Vaishnav, F. Herrmann, D. Shoemaker, and P. Laguna, *Phys. Rev. D* **77**, 081502 (2008).
  - [10] E. Barausse and L. Rezzolla, *Astrophys. J. Lett.* **704**, L40 (2009).
  - [11] F. Pannarale, [arXiv:1208.5869](https://arxiv.org/abs/1208.5869).
  - [12] E. Nakar, *Phys. Rep.* **442**, 166 (2007).
  - [13] W. H. Lee and E. Ramirez-Ruiz, *New J. Phys.* **9**, 17 (2007).
  - [14] L. Rezzolla, B. Giacomazzo, L. Baiotti, J. Granot, C. Kouveliotou, and M. A. Aloy, *Astrophys. J.* **732**, L6 (2011).
  - [15] B. Giacomazzo, R. Perna, L. Rezzolla, E. Troja, and D. Lazzati, *Astrophys. J.* **762**, L18 (2013).
  - [16] P. Marronetti and S. L. Shapiro, *Phys. Rev. D* **68**, 104024 (2003).
  - [17] T. W. Baumgarte and S. L. Shapiro, *Phys. Rev. D* **80**, 064009 (2009).
  - [18] W. Tichy, *Phys. Rev. D* **84**, 024041 (2011).
  - [19] W. Tichy, *Phys. Rev. D* **86**, 064024 (2012).
  - [20] D. Alic, C. Bona-Casas, C. Bona, L. Rezzolla, and C. Palenzuela, *Phys. Rev. D* **85**, 064040 (2012).
  - [21] D. R. Lorimer, *Living Rev. Relativity* **11**, 8 (2008).
  - [22] L. Bildsten, D. Chakrabarty, J. Chiu, M. H. Finger, D. T. Koh, R. W. Nelson, T. A. Prince, B. C. Rubin, D. M. Scott, M. Stollberg, B. A. Vaughan, C. A. Wilson, and R. B. Wilson, *Astrophys. J. Suppl. Ser.* **113**, 367 (1997).
  - [23] D. A. Brown, I. Harry, A. Lundgren, and A. H. Nitz, *Phys. Rev. D* **86**, 084017 (2012).
  - [24] E.ourgoulhon, P. Grandclement, K. Taniguchi, J.-A. Marck, and S. Bonazzola, *Phys. Rev. D* **63**, 064029 (2001).
  - [25] L. Baiotti, T. Damour, B. Giacomazzo, A. Nagar, and L. Rezzolla, *Phys. Rev. D* **84**, 024017 (2011).
  - [26] E. Schnetter, S. H. Hawley, and I. Hawke, *Classical Quantum Gravity* **21**, 1465 (2004).
  - [27] T. W. Baumgarte and S. L. Shapiro, *Phys. Rev. D* **59**, 024007 (1999).
  - [28] M. Alcubierre, *Introduction to 3 + 1 Numerical Relativity* (Oxford University, New York 2008).
  - [29] D. Hilditch, S. Bernuzzi, M. Thierfelder, Z. Cao, W. Tichy, and B. Brüggmann, [arXiv:1212.2901](https://arxiv.org/abs/1212.2901).
  - [30] W. Kastaun, *Phys. Rev. D* **84**, 124036 (2011).
  - [31] A. Ashtekar, C. Beetle, and J. Lewandowski, *Phys. Rev. D* **64**, 044016 (2001).
  - [32] O. Dreyer, B. Krishnan, D. Shoemaker, and E. Schnetter, *Phys. Rev. D* **67**, 024018 (2003).
  - [33] S. A. Hayward, *Phys. Rev. D* **74**, 104013 (2006).
  - [34] L. Rezzolla, L. Baiotti, B. Giacomazzo, D. Link, and J. A. Font, *Classical Quantum Gravity* **27**, 114105 (2010).